Supporting information:

Deactivation mechanism of hydrotalcite-derived Ni-AlOx catalysts during low-temperature CO_2 methanation via Ni-hydroxide formation and the role of Fe in limiting this effect

Chalachew Mebrahtu[†,‡*] Siglinda Perathoner[†], Gianfranco Giorgianni[†], Shiming Chen[†,‡], Gabriele Centi[†], Florian Krebs[‡,§], Regina Palkovits[‡,§], Salvatore Abate[†,*]

[†] Depts. MIFT and ChimBioFarAM (Industrial Chemistry), University of Messina, ERIC aisbl and INSTM/CASPE, V.le F. Stagno D'Alcontres 31, 98166 Messina, Italy.

[‡] Lehrstuhl für Heterogene Katalyse und Technische Chemie, Institut für Technische und Makromolekulare Chemie (ITMC) RWTH Aachen University, Worringerweg 2, 52074 Aachen, Germany.

[§] JARA Energy, Competence Center Power to Fuel RWTH Aachen University Schinkelstraße 2, 52062 Aachen, Germany.

* Corresponding author: abates@unime.it; Asmelash@itmc.rwth-aachen.de;

Post reaction characterizations

XRD patterns

The XRD patterns of the catalysts after extended tests are shown in figure S1, and compared with the reduced one, which after passivation treatment performed in a mixture of 2%Air in N_2, show a small peak of NiO at 2θ =37.3°. The latter peak is instead not observed in all the spent catalysts. Table S1 show the average crystallite size evaluated by Scherrer's law, that are in line with those one obtained by TEM. A shift in the peak attributed to the metallic Ni (51.8°) was not observed and the values for both catalysts were similar, which means even after reduction no Ni-Fe alloy formation was observed. The latter is more evident in the XRD pattern performed in a 2θ range 47-56°.

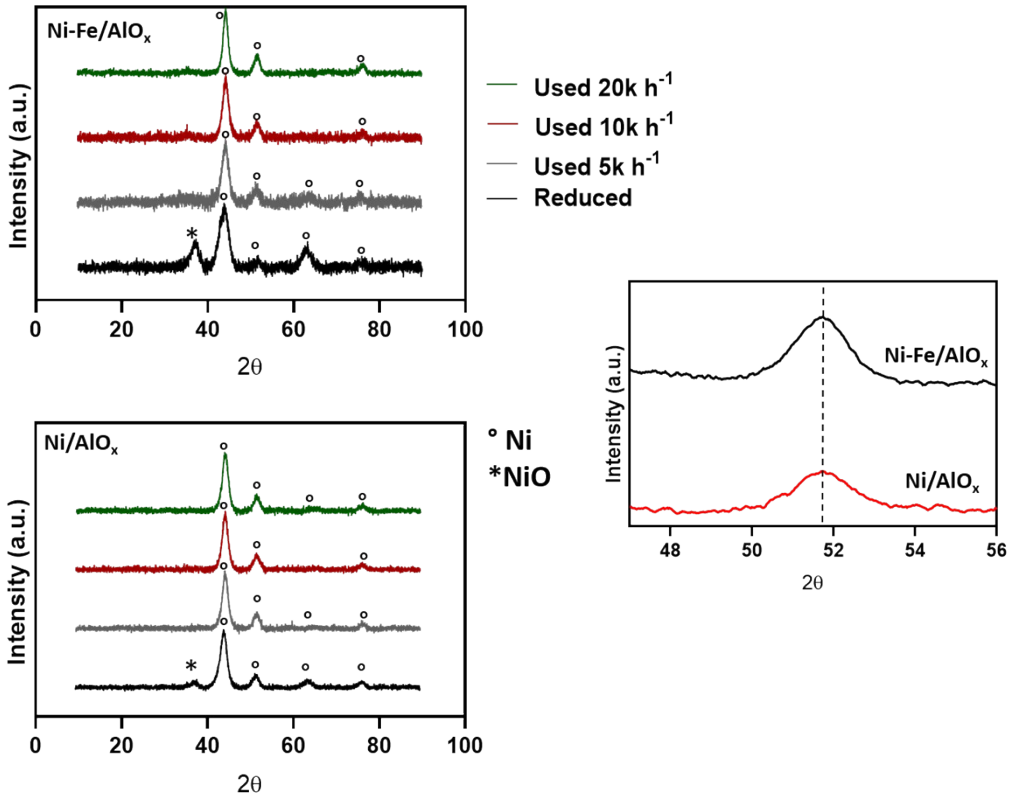

Figure S1. XRD patterns for the catalysts after extended catalytic tests at different GHSVs compared with those of the reduced catalyst (Passivated)

Table S1. Average crystallite size calculated by Scherrer's equation

Catalyst	**Average crystallite size [nm]**			
	Reduced 500°C/H_2 flow	**Used 5k h^{-1}**	**Used 10k h^{-1}**	**Used 20 k h^{-1}**

Ni/AlO_x	5.8	6.1	5.1	6.2
$Ni\text{-}Fe/AlO_x$	5.6	5.5	6.1	6.0

TEM

TEM micrographs of used catalysts at 5k h^{-1} are reported in Figure S2. Dispersed Ni round-shaped nanoparticles can be observed after reaction, excluding any sintering effect. Similar results are obtained also for all the spent catalysts and are not reported here for conciseness.

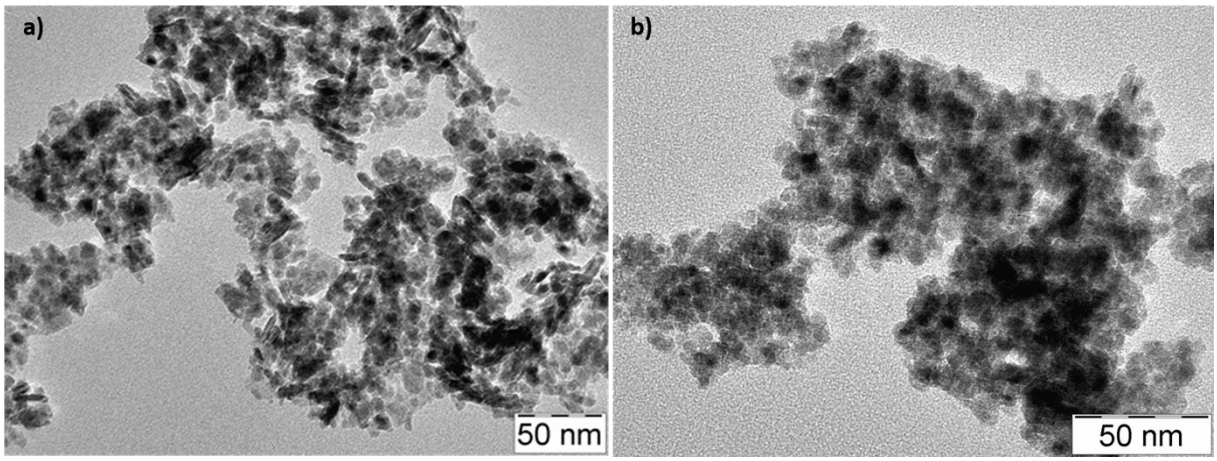

Figure S2. TEM images of catalysts after extended catalytic tests at 5K h^{-1} a) Ni/AlO_x b) Ni-Fe /AlO_x

Raman spectrum of spent catalyst

Raman spectroscopy was also used to deeply investigate the nature and type of carbon deposited on the spent catalysts. For conciseness only $Ni\text{-}Fe/AlO_x$ is reported in figure S3, the same trend was observed for the Ni/AlO_x catalyst

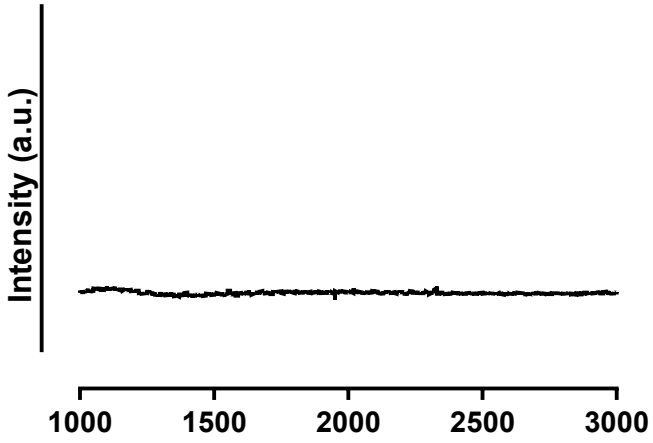

Figure S3. Raman spectrum of Ni-Fe/AlO_x catalyst after extended tests at 5k h^{-1}

XPS analysis

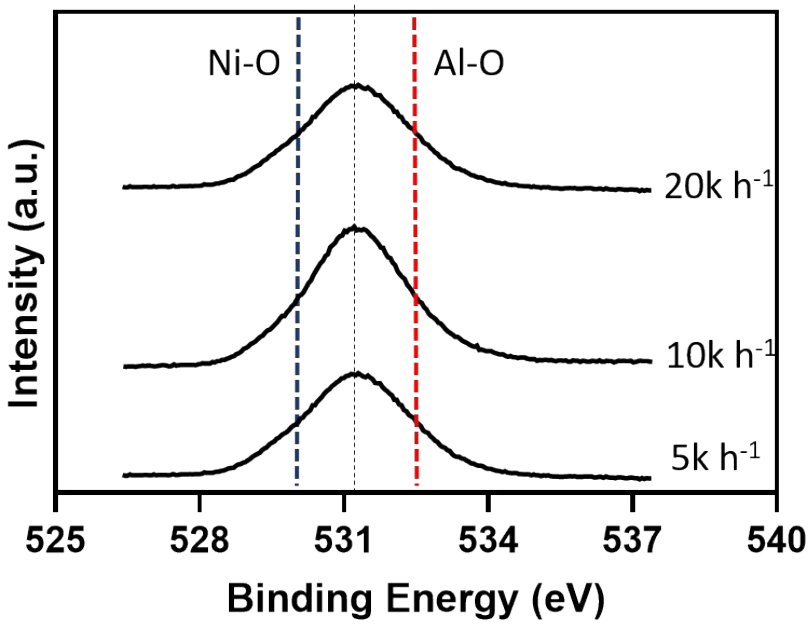

Figure S4. Comparison of the O1s region XPS spectra obtained for the samples after the long-term reaction for the Ni-Fe/AlO_x catalyst at GHSV of 5k h^{-1}, 10k h^{-1} and 20k h^{-1}.

Testing

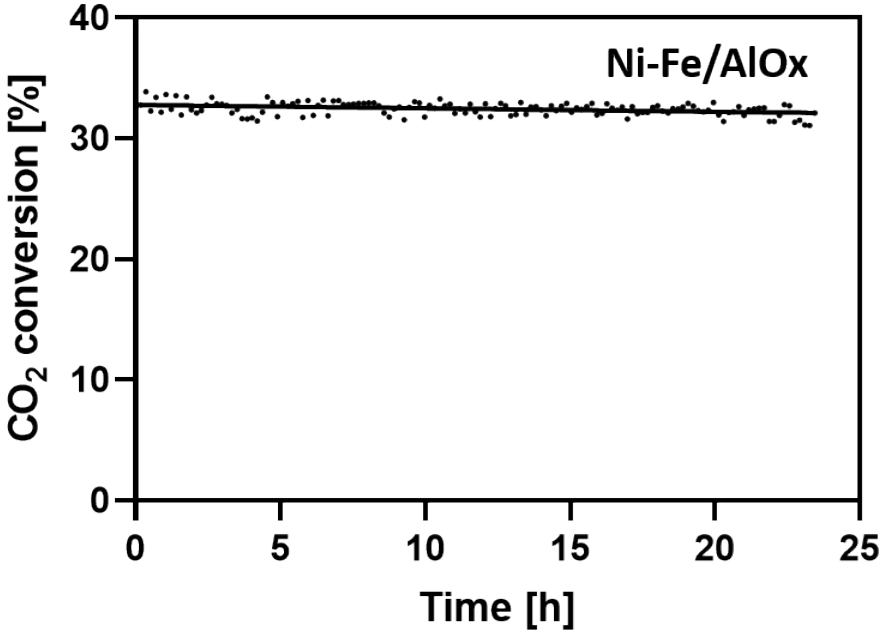

Figure S5. Catalytic performance of Ni-Fe/AlOx catalyst at 300°C and 5 bar and GHSV of 5k h^{-1}, by using 30 mg of catalyst.